Formation of Silver Nanoparticles from a *N*-Hexadecylethylenediamine Silver Nitrate Complex

Abhijit Manna,[†] Toyoko Imae,*[,†] Masayasu Iida,[‡] and Naoko Hisamatsu[‡]

Research Center for Materials Science, Nagoya University, Nagoya 464-8602, Japan, and Department of Chemistry, Faculty of Science, Nara Women's University, Nara 630-8506, Japan

Received March 13, 2001. In Final Form: July 6, 2001

We report the capability for forming silver nanoparticles from a single source of *N*-hexadecylethylenediamine silver nitrate complex that acts as both a metal ion provider and a particle protector. The formation of the metal−ligand complex and nanocomposite is evident from the similarity of a Fourier transform infrared spectrum of free *N*-hexadecylethylenediamine to those of the complex and the composite. The formation and size of particles have been determined from the UV−vis plasmon absorption spectroscopic and transmission electron microscopic (TEM) analyses, respectively. The average particle size is 7.0 ± 1.0 to 12.1 ± 2.9 nm depending on the complex concentration. The TEM photograph shows a two-dimensional array of these particles with an average edge−edge spacing between silver cores of 3.8−3.9 nm (close to double the *N*-hexadecylethylenediamine chain length) after drying the solution. The small-angle X-ray scattering (SAXS) spectrum supports the array of the nanoparticles. The closest center-to-center distance (calculated from the first scattering peak of the SAXS spectrum) between neighboring particles is in agreement with the TEM result. The large edge−edge spacing between cores, in comparison with those of C_{14-18} alkanethiol- and fatty acid-protected nanoparticles which are usually shorter than the alkyl chain length, is due to the dense packing of the diamine monolayer on a metal core and induces a weak interaction force between neighboring particles. Such weak interaction is very important in designing the nanotechnology based on nanoparticles. The colloidal solution of diamine-protected silver nanoparticles is free from flocculation or aggregation for several months.

Introduction

Metal nanoparticles stabilized by self-assembled monolayers are generally prepared according to the method demonstrated first by Brust et al.[1] Most workers have focused on colloidal metals which are stabilized by *n*-alkanethiol. On the other hand, it has been shown that the interaction of amine groups with metal surfaces yields stable colloids.[2] Metal colloids have also been stabilized by ammonium functional groups present in polyelectrolytes and surfactants.[3]

Metal complexes have potential applications in monolayers,[4a] Langmuir−Blodgett films,[4b−d] catalysis,[5a,b] sensors,[5c] microelectronic devices,[5d,e] supramolecular chemistry,[5f,g] and many others.[6] However, the capability of the formation of the metal nanoparticle using a metal complex, which acts as both a metal ion provider and a particle stabilizer, has scarcely been found in the literature.

We develop the route in the synthesis of silver nanoparticles passivated with a surfactant, *N*-hexadecylethylenediamine. In this synthesis procedure, we use a *N*-hexadecylethylenediamine silver nitrate ($Ag(hexd\text{-}en)_2NO_3$) complex. This complex in the crystalline state is synthesized from silver nitrate and *N*-hexadecylethylenediamine ($C_{16}H_{33}NHCH_2CH_2NH_2$, hexd-en). Nanocomposite, diamine-protected silver particles prepared from such a complex are expected to be completely free from the surface contamination caused by the conventional phase-transfer agent.[1]

Experimental Section

Synthesis of *N*-Hexadecylethylenediamine Silver Nitrate Complex, $Ag(hexd\text{-}en)_2NO_3H_2O$. The complex was synthesized similar to the synthesis of $Zn(oct\text{-}en)_2Cl_2$ as reported elsewhere.[7] A solution of 350 mg of hexd-en in 18 cm^3 of water:ethanol (2:3 in volume) mixture was added with stirring to a solution of 48 mg of $AgNO_3$ in 18 cm^3 of water:ethanol (2:3 in volume) mixture. The stirring was continued for ∼2 h. The final

* Corresponding author. E-mail: imae@nano.chem.nagoya-u.ac.jp. Fax: + 81-52-789-5912. Tel: + 81-52-789-5911.

[†] Nagoya University.

[‡] Nara Women's University.

(1) Brust, M.; Walker, M.; Bethell, D.; Schiffrin, D. J.; Whyman, R. *J. Chem. Soc., Chem. Commun.* **1994**, 801.

(2) (a) Xu, C.; Sun, L.; Kepley, L. J.; Crooks, R. M. *Anal. Chem.* **1993**, *65*, 2102. (b) Leff, D. V.; Brandt, L.; Heath, J. R. *Langmuir* **1996**, *12*, 4723. Zhou, M.; Sun, L.; Crooks, R. M. *J. Am. Chem. Soc.* **1998**, *120*, 4877. (c) Esumi, K.; Suzuki, A.; Aihara, N.; Usui, K.; Torigoe, K. *Langmuir* **1998**, *14*, 3157. (d) Manna, A.; Imae, T.; Aoi, K.; Okada, M.; Yogo, T. *Chem. Mater.* **2001**, *13*, 1674.

(3) (a) Berry, C. R.; Skillman, D. C. *J. Appl. Phys.* **1971**, *42*, 2818. (b) Hirai, H. *J. Macromol. Sci., Chem.* **1979**, *A13*, 633. (c) Ahmadi, T. S.; Wang, Z. L.; Green, T. C.; Aenglein, A.; El-Sayed, M. A. *Science* **1996**, *272*, 1924. Lee, P. C.; Meisel, D. J. *J. Phys. Chem.* **1997**, *11*, 2151. (d) Manna, A.; Kulkarni, B. D.; Bondoypadhayay, K.; Vijayamohanan, K. *Chem. Mater.* **1997**, *9*, 3032. (e) Hirai, T.; Watanabe, T.; Komasawa, I. *J. Phys. Chem. B* **1999**, *103*, 10120. (f) Qi, L.; Colfen, H.; Antonietti, M. *Angew. Chem., Int. Ed.* **2000**, *39*, 604.

(4) (a) Tieke, B. *Adv. Mater.* **1990**, 2, 222. (b) Roberts, G. *Langmuir−Blodgett Films*; Plenum: New York, 1990. (c) Zarges, W.; Hall, J.; Lehn, J.-M.; Bolm, C. *Helv. Chim. Acta* **1991**, *74*, 1843. (d) Deschenaux, R.; Masoni, C.; Stoeckli-Evans, H.; Vaucher, S.; Ketterer, J.; Stieger, R.; Weisenhorn, A. L. *J. Chem. Soc., Dalton Trans.* **1994**, 1051.

(5) (a) Richaed, M. A.; Deutsch, J.; Whitesides, G. M. *J. Am. Chem. Soc.* **1979**, *100*, 6613. (b) Murray, R. W. *Acc. Chem. Res.* **1980**, *13*, 135. (c) Zhao, M.; Tokuhisa, H.; Crooks, R. M. *Angew. Chem., Int. Ed. Engl.* **1997**, *36*, 2596. (d) Werkman, P. J.; Wieringa, R. H.; Vorenkamp, E. J.; Schouten, A. J. *Langmuir* **1998**, *14*, 2119. (e) Jaeger, D. J.; Reddy, V. B.; Arulsamy, N.; Bohle, D. S. *Langmuir* **1998**, *14*, 2589. (f) Lehn, J.-M. *Supramolecular Chemistry*; VHC: New York, 1995. (g) Imae, T.; Ikeda, Y.; Iida, M.; Koine, N.; Kaizaki, S. *Langmuir* **1998**, *14*, 5631.

(6) (a) Reynolds, G. A.; Drexhage, K. H. *J. Appl. Phys.* **1975**, *46*, 4852. (b) Verdaguer, M. *Science* **1996**, *272*, 698. (c) Sato, O.; Lyoda, T.; Fujishima, A.; Hashimoto, K. *Science* **1996**, *272*, 704. (d) Cummings, S. D.; Cheng, L.-T.; Eisenberg, R. *Chem. Mater.* **1997**, *9*, 195. (e) Hill, C. A. S.; Carlton, A.; Underhill, A. E.; Malik, K. M. A.; Hoursthouse, M. B.; Karaulov, A. I.; Oliver, S. N.; Kershaw, S. V. *J. Chem. Soc., Dalton Trans.* **1998**, *3*, 334.

10.1021/la010389j CCC: $20.00
Published on Web 08/23/2001

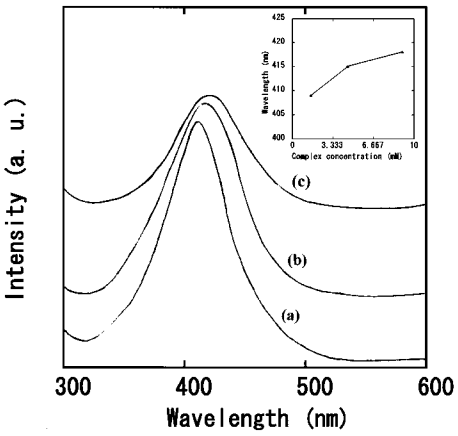

Figure 1. UV−vis absorption spectra of *N*-hexadecylethylenediamine-protected silver nanoparticles in *n*-heptane. The complex concentrations are (a) 1.5, (b) 4.5, and (c) 9.0 mM. The spectra are presented with shifting in the vertical axis. The inset figure shows a plot of UV−vis absorption maximum vs complex concentration.

reaction composition was a 1:3 molar ratio of metal salt/hexd-en. After evaporation of the solvent, the crude $Ag(hexd\text{-}en)_2NO_3H_2O$ complex was extracted into chloroform from the water/chloroform system and recrystallized from ethanol solution (yield ∼ 55%). The purity of the crystal was determined by an elemental analysis. (Anal. Found: C, 56.97%; H, 10.91%; N, 9.42%. Calcd: C, 57.12%; H, 10.92%; N, 9.25%.)

Synthesis of Diamine-Protected Silver Nanoparticle. The nanoparticle was synthesized by a two-phase redox reaction, which was carried out in the *n*-heptane/water system using sodium borohydride as a reducing agent. Five cm^3 of a *n*-heptane solution of $Ag(hexd\text{-}en)_2NO_3$ (1.5, 4.5, or 9 mM) and 5 cm^3 of a freshly prepared solution of $NaBH_4$ (15, 45, or 90 mM) were mixed together and stirred vigorously for ∼2 h. Subsequently, the mixture was allowed to separate into two distinct transparent phases. A deep-yellow *n*-heptane phase was in equilibrium with a colorless aqueous phase. The *n*-heptane phase was separated and used for the characterization of nanoparticles. The colloidal solution of the nanoparticle in *n*-heptane was free from flocculation or aggregation for several months.

Characterization. Optical measurements were carried out at room temperature on a Shimadzu UV 2200 UV−vis spectrometer using a quartz cell (10 mm path). The spectra were subtracted by the background UV−vis spectra of the same solvent mixture.

Fourier transform infrared (FT-IR) spectra in the region of 3500−1000 cm^{-1} were recorded at room temperature on a Bio-Rad FTS 575C FT-IR instrument. A specimen for the analysis was prepared as a KBr pellet of dry composite material (obtained by the evaporation of solvent from the colloidal solution).

A specimen for the transmission electron microscopy (TEM) was prepared by spreading a small drop of approximately 20 times dilute colloidal solution onto a standard copper grid (coated with a thin amorphous Formver carbon film) and letting the drop dry completely in air. The particle size and morphology were observed at room temperature on a Hitachi H-800 electron microscope operating at 100 kV. The size distribution was derived from histograms for about 200 particles.

Small-angle X-ray scattering (SAXS) data were recorded at room temperature on a Rigaku instrument (SAX-LPB) using an imaging plate. The X-ray radiation source (Cu Kα, $\lambda = 0.154$ nm) was operated at 45 kV and 100 mA. The specimen was prepared as a dry cast film on a 10 μm thin Capton film. Scattering of the nanoparticle-free Capton film was subtracted as a background scattering. The X-ray radiation times were 270 and 60 min for diamine- and thiol-protected nanoparticles, respectively. The solution of diamine-protected silver nanoparticles prepared from 1.5 mM complex solution was used for SAXS experiments. The thiol-protected silver nanoparticle was prepared in a Winsor II type microemulsion.[3d]

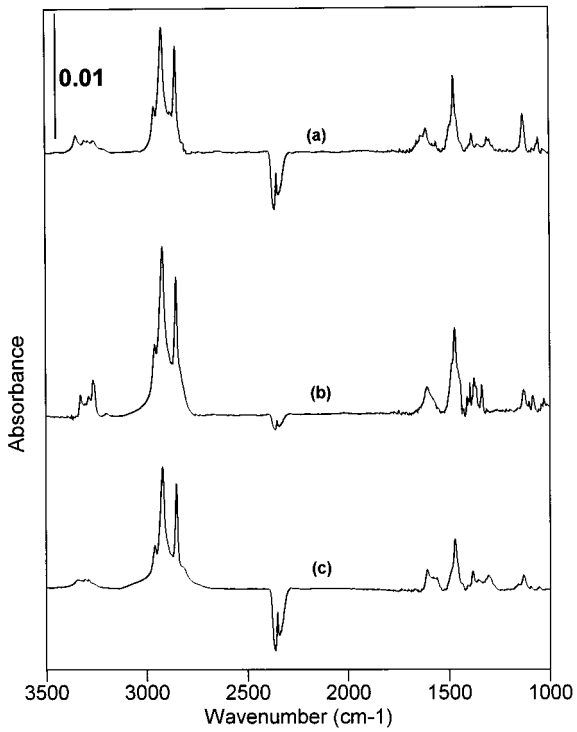

Figure 2. Comparison of the FT-IR spectra at 3500−1000 cm^{-1}: (a) free *N*-hexadecylethylenediamine, (b) silver complex, and (c) *N*-hexadecylethylenediamine-protected silver nanoparticles.

Table 1. Characteristic Data for *N*-Hexadecylethylenediamine-Protected Nanoparticles

complex concn in *n*-heptane soln (in mM)	UV−vis absorption max (λ_{max}) (in nm)	av particle diam (in nm)	std dev	edge-edge sepn between particle cores (in nm)
1.5	409	7.0	±1.0	3.8
4.5	413	10.3	±2.3	3.9
9.0	422	12.1	±2.9	3.8

Results and Discussion

Formation of Particles. Figure 1 shows UV−vis absorption spectra of ligand-protected silver nanoparticles in *n*-heptane. The colloidal solution having the lowest concentration, 1.5 mM, displays a strong absorption band at 409 nm (Figure 1a), which can be assigned to the surface plasmon absorption of silver clusters. Metallic silver is known to have an intense plasmon absorption band in the visible region.[7] The electronic energy levels and the optical transition in the "roughened" silver surface have been extensively studied by several groups. It was confirmed that the Ag 4d to 5sp interband transition generally occurs around an energy corresponding to 320 nm.[8] The characteristic red shift of the plasmon absorption band supports the formation of diamine-protected silver "quantum-dot" nanoparticles.

The inset shown in Figure 1 is a plot of wavelength of UV−vis absorption maximum versus concentration of the diamine−silver complex. The plot shows the variation of the peak maximum from 409 nm at 1.5 mM to 422 nm at

(7) (a) Iida, M.; Yonezawa, A.; Tanaka, J. *Chem. Lett.* **1997**, 663. (b) Iida, M.; Tanase, T.; Asaoka, N. *Chem. Lett.* **1998**, 1275. (c) Iida, M.; Er, H.; Hisamatsu, N.; Tanase, T. *Chem. Lett.* **2000**, 518. (d) Ikeda, Y.; Imae, T.; Hao, J.-C.; Iida, M.; Kitano, T.; Hisamatsu, N. *Langmuir* **2000**, *16*, 7618.

(8) (a) Kreibig, U. *J. Phys. F*: *Metal Phys.* **1974**, *4*, 999. (b) Henglein, A. *J. Phys. Chem.* **1993**, *97*, 5457. (c) Zhao, M.; Crooks, R. M. *Angew. Chem., Int. Ed.* **1999**, *38*, 364.

Table 2. FT-IR Bands for Free *N*-Hexadecylethylenediamine, Complex, and Nanoparticles

assignment	band position[a] in cm^{-1}		
	free diamine	diamine−silver complex	silver nanoparticle
NH_2 antisymmetric and symmetric stretching, NH stretching, and one overtone	3345 (m)	3325 (m)	3340 (vw)
	3303 (vw)	3315 (vw)	3304 (vw)
	3285(vw)	3284 (w)	3285 (vw)
	3257 (w)	3262 (m)	3255 (sh)
CH_3 asymmetric stretching	2957 (m)	2956 (m)	2958 (m)
CH_2 antisymmetric stretching	2919 (vs)	2917 (vs)	2919 (vs)
CH_3 symmetric stretching	2877 (w)	2876 (sh)	2877 (sh)
CH_2 symmetric stretching	2851 (vs)	2850 (vs)	2850 (vs)
NH_2 and NH deformation	1608 (m)	1604 (m)	1606 (m)
	1559 (vw)	1562 (sh)	1559 (sh)
CH_2 scissoring	1471 (s)	1468 (s)	1469 (s)
		1408 (sh)	
CH_2 wagging	1382 (m)	1392 (m)	1382 (w)
		1372 (m)	
		1334 (m)	
CH_3 bending (U type)	1307 (w)	1311 (vw)	1303 (w)
CH_2 twisting	1129 (m)	1127 (w)	1129 (w)
		1081 (w)	
C−C stretching and NH_2 wagging	1052 (w)	1026 (vw)	

[a] Very strong (vs), strong (s), medium (m), weak (w), very weak (vw), and shoulder (sh).

9 mM (see also Table 1). Furthermore, Figure 1 shows that the absorption maximum broadens with increasing the concentration.

Metal−Ligand Complex Formation and Particle Encapsulation. Figure 2 shows a comparison of the FT-IR spectra (3500−1000 cm^{-1}) for (a) the free ligand, (b) the metal−ligand complex, and (c) the composite nanoparticles. The band positions and their assignments are listed in Table 2. All characteristic bands of the ligand[9,10] are clearly seen. It is confirmed from the similarity in the features of the three spectra that the ligand is an essential component of both the complex and the composite nanoparticles.

The bands at 3345, 3303, 3285, and 3257 cm^{-1} are assigned to the NH_2 antisymmetric and symmetric stretching, NH stretching, and one-overtone modes. The position and relative intensity of these bands changed during complex formation and adsorption on the metal particle. For example, the shifts of the band at 3345 cm^{-1} to lower wavenumber (3325 and 3340 cm^{-1}) were observed for the $Ag(hexd\text{-}en)_2NO_3$ complex crystal and metal nanocomposite. These shifts indicate the preferable arrangement of hexd-en in the complex crystal and on the metal particle surface. The larger band shift for the complex crystal indicates a stronger interaction between the metal ion and amine group. The absorption bands at 3303 and 3257 cm^{-1} show small shifts to higher wavenumbers (3315 and 3262 cm^{-1}, respectively) in a spectrum of the $Ag(hexd\text{-}en)_2NO_3$ complex, while these band positions seem to be invariant with respect to the adsorption on the nanoparticle. The absorption band position at 3285 cm^{-1} remained unchanging for the $Ag(hexd\text{-}en)_2NO_3$ complex and composite nanoparticles. Similar invariants or slight shifts were observed for NH_2 and NH deformation bands at 1608 and 1559 cm^{-1}. The band at 1052 cm^{-1}, which is assigned to the C−C stretching vibration mode overlapped with NH_2 wagging, shows a low-wavenumber shift with an intensity decrease due to complex formation and adsorption on the nanoparticle.

The peak positions of CH_3 asymmetric (2957 cm^{-1}) and symmetric (2877 cm^{-1}) stretching, CH_2 antisymmetric (2919 cm^{-1}) and symmetric (2851 cm^{-1}) stretching, CH_2 scissoring (1471 cm^{-1}), CH_3 bending (1307 cm^{-1}), and CH_2 twisting (1129 cm^{-1}) vibrational modes are invariant with respect to the complex formation and adsorption on the nanoparticle. It is suggested from the band positions and their invariance that the alkyl chains always take the stretched (trans) conformation irrespective of the complex formation and adsorption. The CH_2 wagging vibration band at 1382 cm^{-1} split into bands at 1392 and 1372 cm^{-1} during the complex formation. We also observe progressive bands at 1408, 1334, and 1081 cm^{-1} in the spectrum of the complex crystal. Such a band splitting and the band progression between 1400 and 1000 cm^{-1} indicate the preferred arrangement of diamine in the complex crystal.[10b] The variation of infrared absorption bands, especially NH and NH_2 bands, between the complex crystal and the metal nanoparticles suggests the formation of ligand-encapsulated nanoparticles and the structural variation of hexd-en. The structure of the diamine group on the metal nanoparticle is rather like a free diamine.

Particle Size. The size of nanoparticles prepared from solutions of the metal−ligand complex at different concentrations was examined by TEM. Typical bright field TEM photographs and histograms of the size distribution are shown in Figure 3. The photographs show that all of the particles are almost spherical. The average size, standard deviation,[2d] and edge−edge separation between the particle cores at different concentrations of the complex are given in Table 1. The average particle size increases from 7.0 ± 1.0 to 12.1 ± 2.9 nm with increasing concentration of the complex from 1.5 to 9.0 mM. From Table 1, the red shift and the broadening of the plasmon absorption band with increasing concentration of the complex relate to the increase in particle size and its polydispersity.

The TEM photographs also show that the ligand-coated particles taking part in the formation of nanoscale structure maintain less aggregation of metal cores into flocs. The nanoscale structure follows the formation of a well-defined monolayer in a two-dimensional (2D) hexagonal array. The formation of the best-defined monolayer with keeping a constant edge−edge spacing between silver cores was observed for the particles of minimum size, as seen in Figure 3a. The edge−edge separation between

(9) (a) Dollish, F. R. *Characteristic Raman Frequencies of Organic Compounds*; J. Wiley: New York, 1974. (b) Bellamy, L. J. *The Infrared spectra of Complex Molecules*; J. Wiley: New York, 1975.

(10) (a) Nuzzo, R. G.; Duboli, L. H.; Allara, D. L. *J. Am. Chem. Soc.* **1990**, *112*, 555. (b) Myrzakozha, D. A.; Hasegawa, T.; Nishijo, J.; Imae, T.; Ozaki, Y. *Langmuir* **1999**, *15*, 6890.

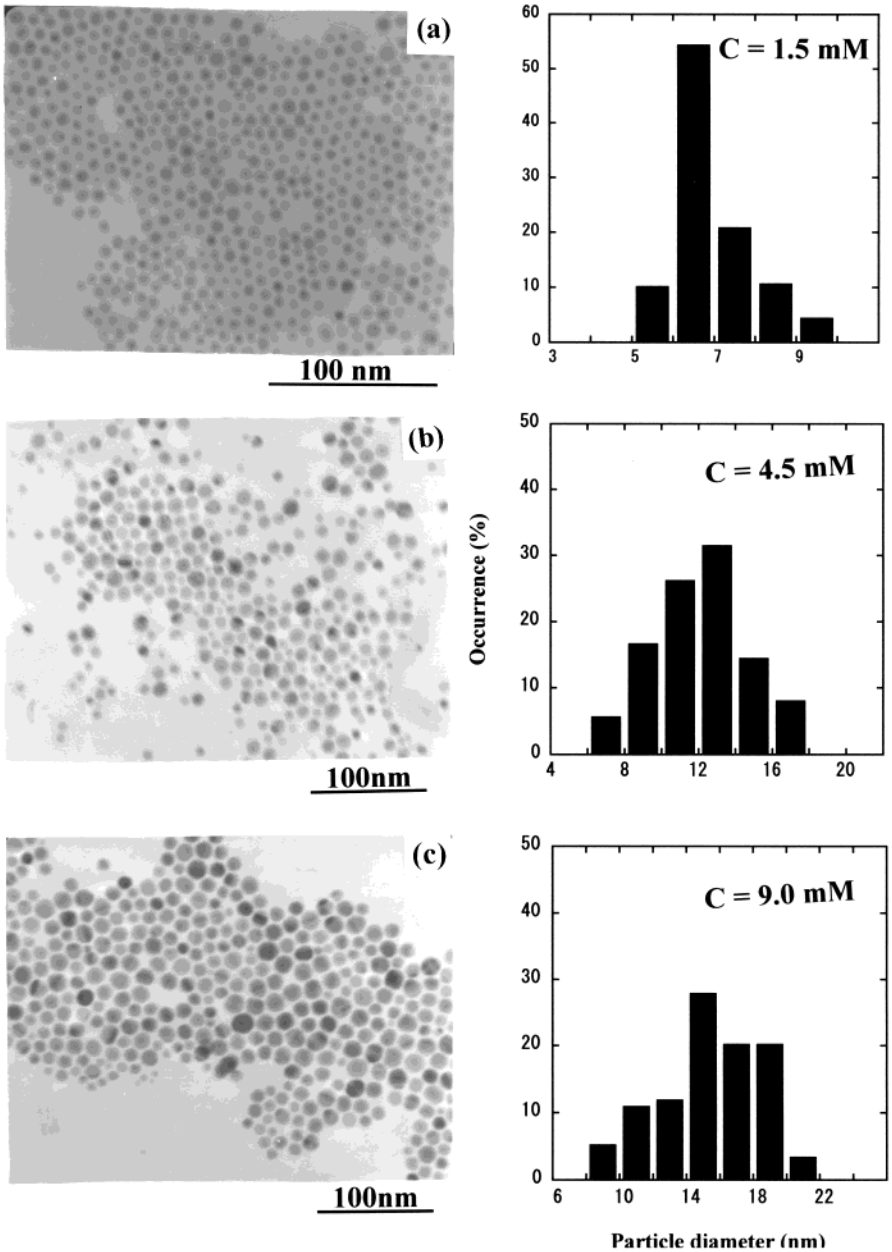

Figure 3. TEM photographs (left-hand side) and particle size distributions (right-hand side) of *N*-hexadecylethylenediamine-protected silver nanoparticles. The complex concentrations on the nanoparticle preparation are (a) 1.5, (b) 4.5, and (c) 9.0 mM in *n*-heptane.

particle cores (3.8−3.9 nm, see Table 1) does not change with particle size and is nearly double the extended chain length of *n*-hexadecane or the *n*-hexadecyl moiety.[10,11] The extended chain conformation was supported by the infrared absorption. Then, the intercore spacing is suggested to arise from the bilayer formation of the alkyl chains between neighboring particles during the formation of the 2D monolayer, as illustrated in Figure 4a.

The edge−edge spacing between cores of C_{14-18} alkanethiol-capped nanoparticles is usually shorter than the length of the corresponding single chain.[11] This was explained in consideration of the interdigitation between alkane chains (see Figure 4b). A similar type of interdigitated monolayer was reported for fatty acid in the literature.[12] Large edge−edge spacing between cores (compared with the alkanethiol-protected particles) was observed in the 2D monolayer of diamine-protected silver nanoparticles. The large separation is due to the dense-packed monolayer of diamines on metal cores, and this causes the weaker interaction between neighboring particles.

2D Ordering of Particles. The crystal with hexagonal structure usually shows several SAXS peaks. The position of these peaks on the scattering vector *Q*-axis obeys the relationship $1:3^{0.5}:2:7^{0.5}$ and so forth.[13] Figure 5 shows the SAXS spectra of the cast films of (a) diamine-protected

(11) Motte, L.; Pileni, M. P. *J. Phys. Chem. B* **1998**, *102*, 4104.

(12) (a) Bayerl, T. M.; Bloom, M. *Biophys. J.* **1990**, *58*, 357. (b) Wooding, A.; Kilner, M.; Lambrick, D. B. *J. Colloid Interface Sci.* **1991**, *144*, 236. (c) Ward, R. N.; Duffy, D. C.; Davies, P. B.; Baib, C. D. *J. Phys. Chem.* **1994**, *98*, 8536. (d) Sackmann, E. *Science* **1996**, *271*, 43. (e) Patil, V.; Mayya, K. S.; Pradhan, S. D.; Sastry, M. *J. Am. Chem. Soc.* **1997**, *119*, 9281. (f) Kung, L. A.; Kam, L.; Hovis, J.; Boxer, G. S. *Langmuir* **2000**, *16*, 6773.

(13) (a) Wu, G.; Chu, B.; Schneider, D. K. *J. Phys. Chem.* **1994**, *98*, 12018. (b) Alexandridis, P.; Olsson, U.; Lindman, B. *Macromolecules* **1995**, *28*, 7700. (c) Svensson, B.; Alexandridis, P.; Olsson, U. *J. Phys. Chem.* **1999**, *102*, 7541. (d) Svensson, B.; Olsson, U.; Alexandridis, P. *Langmuir* **2000**, *16*, 6839.

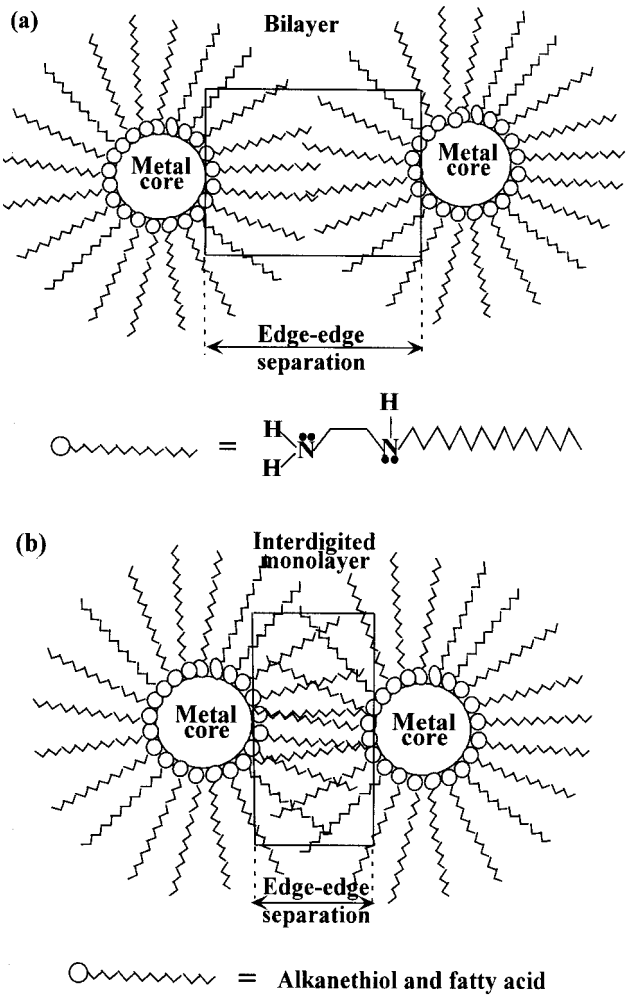

Figure 4. Schematic illustration of nanoparticle structure: (a) the normal bilayer between *N*-hexadecylethylenediamine-protected silver nanoparticles and (b) the conventional interdigitated monolayer between alkanethiol- or fatty acid-protected nanoparticles.

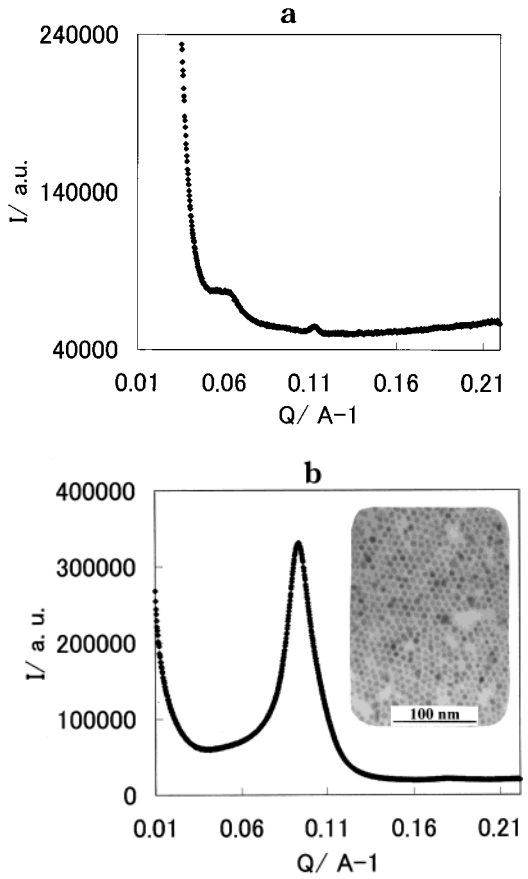

Figure 5. (a) A SAXS spectrum of *N*-hexadecylethylenediamine-protected silver nanoparticles. (b) A SAXS spectrum of dodecanethiol-protected silver nanoparticles. The inset shows a TEM photograph of the same sample.

and (b) dodecanethiol-protected silver nanoparticles. The SAXS spectrum of the diamine-protected particles, Figure 5a, shows two Bragg peaks at $Q = 0.65$ and 1.14 nm^{-1}. Since these two Q-values obey the $1:3^{0.5}$ relationship, they correspond to the reflections of [10] and [11], respectively, of the 2D hexagonal array. In the case of the 2D hexagonal array, the lattice parameter (α, nearest neighbor distance) is calculated from the Bragg equation, $Q_{hk} = 4\pi(h^2 + k^2 + hk)^{0.5}/(3^{0.5}\alpha)$, where Q_{hk} is the 2D scattering vector of the [hk] reflection and h and k are the Miller indices. The lattice parameter α obtained from the Bragg equation is 11.1 nm. This value is very close to the particle center-to-center distance (10.8−10.9 nm) obtained from the TEM experiment.

The SAXS spectrum of the dodecanethiol-protected nanoparticle shows a very strong Bragg peak at $Q = 0.93$ nm^{-1} which corresponds to the reflections of [10] with $\alpha = 7.8$ nm. This denotes that the particles are well ordered. The inset of Figure 5b depicts the TEM photograph of the same sample. The average particle size and particle edge−edge separation are 66 and 1.8 nm, respectively. The α value (7.8 nm) obtained from SAXS is slightly smaller than the center-to-center distance (8.4 nm) between the particles obtained from the TEM experiment for thiol-protected nanoparticles.

The nearly equivalent value of α to the center-to-center distance between the particles for the diamine-protected nanoparticles indicates the preservation of a bilayer between neighboring particles in a cast film on a Capton film. The decrease of the α value from the center-to-center distance for the dodecanethiol-protected nanoparticles implies the formation of the stronger interdigitated monolayer during the preparation of a cast film on a Capton film, revealing the dependence of interdigitation on the nature of the substrate.

Conclusions

The *N*-hexadecylethylenediamine surfactant forms a stable crystalline complex with silver(I) ions. The probable molecular formula of this complex is $Ag(hexd\text{-}en)_2NO_3H_2O$. The complex is capable of forming stable nanoparticles. Use of the metal complex has an advantage over conventional two-phase methods. For example, the absence of a phase-transfer agent avoids the contamination on the particle surface caused by the agent, and the alteration of concentration of the complex in solution easily controls the particle size. This study indicates that the *N*-hexadecylethylenediamine metal complex is very useful for the preparation of 2D monolayers and films (e.g., Langmuir−Blodgett films) of nanoparticles containing metal ions of different valence states (e.g., Ag^+ and Ag^0) and also for the design of nanotechnology based on nanoparticles.

LA010389J